JOURNAL OF APPLIED ELECTROCHEMISTRY 19 (1989) 263–270

Axial dispersion in electrolyte flow through anisotropic packed beds

P. LEGENTILHOMME, J. LEGRAND, J. COMITI

Laboratoire de Génie des Procédés, I.U.T., B.P. 420, 44606 Saint-Nazaire Cedex, France
44606 Saint-Nazaire Cedex, France

Received 16 March 1988; revised 23 July 1988

The axial dispersion of an electrolyte flowing through fixed beds was determined using a polarographic method with two-point measurement. Axial dispersion coefficients at various flow rates were obtained in fixed beds composed of glass beads in order to test the experimental method. Further experiments were performed using square-based parallelipipedic particles (so-called flat plates) defined by the ratio e/a of the thickness, e, over the side, a, of the plate. The influence of the ratio e/a on the axial mixing was studied. The experimental data were expressed in the form of empirical correlations giving the Peclet number as a function of the Reynolds number; these two adimensional numbers were based on the interstitial velocity and the equivalent particle diameter. For the flat plate fixed beds, which form very anisotropic porous media, the axial dispersion was greater (up to a factor of 10) than that obtained in the isotropic porous media of spherical particles. The results were explained by the velocity fluctuations within a cross section.

Nomenclature

a	side of the flat plates
a_{vs}	specific surface area
C	tracer concentration
C', C''_{exp}, C''_{calc}	adimensional tracer concentrations
D	diffusion coefficient
D_{ax}	axial dispersion coefficient in fixed beds
D_{ax_i}	axial dispersion coefficient in the pore i
$d_p = 6/a_{vs}$	equivalent particle diameter
e	thickness of the flat plates
f	friction factor
F_T	transfer function
I_L	limiting diffusional current
k	mass transfer coefficient
L	distance between the two sensors
p	probability of axial displacement
$Pe = uL/D_{ax}$	Peclet number
$Pe_i = ud_p/D_{ax}$	interstitial Peclet number
$Pe = 2\bar{r}u_t/D_{ax}$	pore Peclet number
r_i	radius of the pore i
$\bar{r}$	average pore radius
$Re = u_0 d_p/\nu$	superficial Reynolds number
$Re_i = ud_p/\nu$	interstitial Reynolds number
$Re_t = 2\bar{r}u_t/\nu$	pore Reynolds number
S	surface area of the sensors
$Sc = \nu/D$	Schmidt number
$\bar{t}_s$	mean residence time
u	interstitial velocity
u_0	superficial velocity
$\bar{u}_t$	area-averaged fluid velocity in the pores
$\bar{u}_{ti}$	area-averaged fluid velocity in the pore i

Greek letters

$\gamma = \sigma/\bar{r}$	variation coefficient
$\Delta P/L$	pressure drop per length unit
ε	bed porosity
ν	kinematic viscosity
ϱ	electrolyte density
σ	standard deviation
τ	bed tortuosity

1. Introduction

The importance of packed-bed reactors in the chemical industry has promoted much work on axial dispersion during the last few decades, however, there is no consensus on the modelling of the flow through packed beds, especially for liquid flow.

Mixing in fixed beds is mostly characterized by dispersion models [1], and particularly the axial dispersion model, in which the radial dispersion is neglected. The axial dispersion model is a one-parameter model; non-ideality is considered as a deviation from plug flow caused by fluctuations of local flow velocities which are superimposed on the average plug flow velocity, u, which corresponds to the interstitial velocity in flow through packed beds. These fluctuations are described analogously to Fick's law of diffusion, using the dispersion coefficient, D_{ax}, instead of Fick's diffusion coefficient. The concentration, C, of a tracer injected uniformly over the cross section of a bed of non-porous particles is given as a function of time, t, and axial position, z, by the follow-

0021-891X/89 $03.00 + .12

ing equation:

$$\frac{\partial C}{\partial t} = D_{ax}\frac{\partial^2 C}{\partial z^2} - u\frac{\partial C}{\partial z} \quad (1)$$

The axial dispersion coefficient, D_{ax}, is assumed independent of the concentration and the position z.

Axial dispersion in fixed beds is attributable to the combined effects of molecular and eddy diffusion. For gas flow through fixed beds, Edwards and Richardson [2] proposed the following equation:

$$D_{ax} = 0.73D + \frac{0.5ud_p}{1 + 9.7D/ud_p} \quad (2)$$

where D is the diffusion coefficient and d_p is the particle diameter.

Contrary to the case of gas flow, molecular diffusion in liquid flow can be neglected in comparison with the dispersion phenomenon; this is explained [2] by the difference in the orders of magnitude of the respective molecular diffusivities. Therefore, the dispersion coefficient may be given by the relation $D_{ax} = \frac{1}{2}ud_p$, which corresponds to the eddy diffusion term of Equation 2. In practice, the dispersion coefficients are greater than those calculated by the previous equation. Edwards and Richardson [2] have explained this result by the fact that dispersion is controlled by the laminar flow regime, a situation which rarely occurs in gaseous systems because the influence of the molecular diffusion is important up to moderate values of Reynolds number.

In the review of Wen and Fan [1], it is seen that the dispersion coefficient, in most of the referenced works, can be expressed by:

$$D_{ax} = \alpha u^m \quad (3)$$

with m between 0.8 and 1.2. The parameter α depends on the type of particles constituting the fixed beds. In the literature, most work concerns spherical particle-packed beds, or industrial packings (Rashig rings, Berl saddles, etc.) typically used in mass transfer operations. But there are no results on axial dispersion in liquid flow through fixed bed of anisotropic convex particles.

In this work we have studied axial dispersion in anisotropic packed beds composed of flat plates. This porous medium has been chosen to simulate wood chip bed reactors of the paper-making industry. The flat plate packing could also be used in a volumic electrode, because of its very good mass transfer behaviour [3]. A potential application of these packings is selective metal recovery on metallic turnings. The axial dispersion coefficients, obtained using a polarographic method, are determined as a function of the liquid flow velocity and the geometric parameters of the flat plates.

2. Experimental details

2.1. *General flow apparatus*

A schematic flow diagram of the apparatus is shown in Fig. 1. From the main reservoir, where the solution

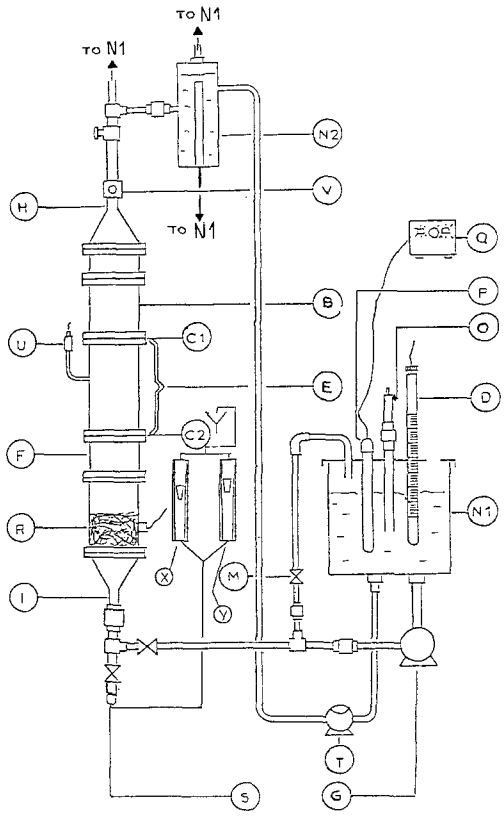

Fig. 1. Diagram of experimental set-up: B, calming section; C1, upper cathode; C2, lower cathode; D, thermometer; E, studied fixed bed; F, calming section; G, centrifugal pump; H, cell inlet; I, cell outlet; M, bypass; N1, main reservoir; N2, constant level reservoir; O, nitrogen inlet; P, heating resistance; Q, temperature regulation; R, anode; S, fluid outlet; T, peristaltic pump; U, reference electrode; V, injection point; X, flowmeters.

is maintained at 25° C, the liquid flows through a peristaltic pump to a constant level taken, and then downward in the column; the volumic flow rate is measured using two rotameters in a range between 0.56 and 18 $cm^3 s^{-1}$. The filling of the column is performed by means of a centrifugal pump, which allows an upward circulation of the solution to avoid the presence of gas bubbles inside the fixed beds. The packed column has an inner diameter, ϕ_c, of 6.0 cm and a total length of 55 cm. The studied fixed beds are composed of three identical parts. The upper part, 10 cm high, is a calming section to allow the flow regime establishment before the first sensor C_1 (Fig. 1). The middle part, with a height L = 15 cm, is included between the two sensors C_1 and C_2 and constitutes the test section. The lower part, with a height l = 5 cm, permits the continuity of the flow after the second sensor. The ratio l/L = 0.33 is sufficiently great to consider the fixed bed as infinite after Wakao *et al.* [4].

The solid particles used as packing materials are of two types: spherical glass beads, 0.5 cm in diameter, and square flat plates. The dimensions of the flat plates (see Table 1) are determined from a sample of 100 particles. The porosity and the specific surface of the different fixed beds are given in Table 1.

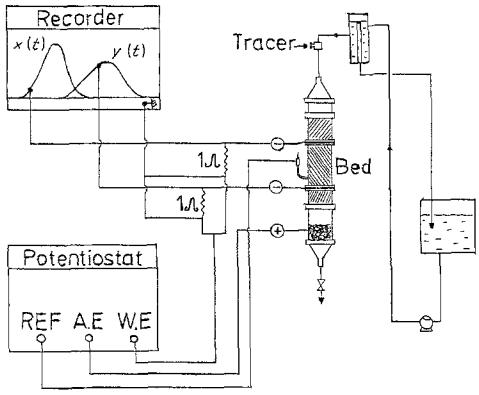

Fig. 2. Schematic diagram of experimental method for the determination of the residence time distribution.

2.2. *Electrochemical method*

The experimental determination of the residence time distribution (RTD) is performed by a polarographic method with a three-electrode circuit (Fig. 2). The cathode consists of two identical nickel grids used as sensors for the determination of the RTD. The anode is a nickel wire knit with a greater surface area than that of the cathode. The reference electrode is made of platinum.

The electrolyte is an aqueous solution of 10^{-3} M potassium ferricyanide, 0.013 M ferrocyanide and 1 M sodium hydroxide. At 25° C, the physical properties of the electrolyte are: density, ϱ, 1043 kg m^{-3} and kinematic viscosity, ν, 1.03 × 10^{-6} m^2 s^{-1}. The tracer is a saturated solution of potassium ferricyanide. After the injection of the tracer, the liquid is not recycled to avoid the modification of the concentrations of the basic solution. The injected tracer quantity is very small, about 0.5–1 cm^3 so the physical properties of the solution and the hydrodynamics inside the fixed bed can be considered as constant during the experiments. The injector is identical to one used in chromatography and is located at the top of the column (Fig. 2). The studied electrochemical reaction is the reduction of the ferricyanide ions. All the experiments have been performed under diffusion-controlled conditions at the cathodes. Consequently, we have the following relation between the limiting diffusion current I_L and the mass transfer coefficient k:

$$I_L = nFkSC \tag{4}$$

where n is the number of electrons transferred in the electrochemical reaction, F is Faraday's constant, S is the cathode surface area and C the potassium ferricyanide concentration. For given hydrodynamic conditions, the mass transfer coefficient, k, is fixed and so the limiting current, I_L, is a linear function of the concentration, C. After the tracer injection, the time change of the concentration is expressed (Equation 4) by the time change of the intensity, I_L. The recording of the curves giving I_L as a function of time on the two sensors C_1 and C_2 permits the determination of the residence time distribution (RTD).

3. Analysis of experimental curves

The determination of the mean residence time and the axial dispersion coefficient is made by using the method of curve fitting in the time domain [4, 5]. This method, which is the most accurate according to Fahim and Wakao [6], is based on the comparison of the experimental response curve with that calculated in the time domain from the transfer function of the dispersed plug flow model.

In Fig. 3 typical experimental input and response signals, $x(t)$ and $y(t)$, obtained with the electrochemical method are shown. The signals $x(t)$ and $y(t)$ are normalized by:

$$C'(t) = \frac{x(t)}{\int_0^{2T} x(t)\,dt} \quad C''_{exp}(t) = \frac{y(t)}{\int_0^{2T} y(t)\,dt} \tag{5}$$

where $2T$ is the time allowing the tail of the response signal $y(t)$ to vanish (Fig. 3). The signals $C'(t)$ and $C''_{exp}(t)$ are expressed in terms of Fourier series. The transfer function $F_T(i\omega)$ is easily found from Equation 1:

$$F_T(i\omega) = \exp\left\{\frac{Pe}{2}\left[1 - \left(1 + \frac{4i\omega}{Pe}\,\bar{t}_s\right)^{1/2}\right]\right\} \tag{6}$$

where Pe is the Peclet number and $\bar{t}_s$ the mean residence time. The predicted response signal $C''_{calc}(t)$ is calculated from the transfer function and the input signal $C'(t)$:

$$F_T(i\omega) = \frac{\int_0^{2T} C''_{calc}(t)\exp(-i\omega t)\,dt}{\int_0^{2T} C'(t)\exp(-i\omega t)\,dt} \tag{7}$$

The comparison of experimental and predicted response signals $C''_{exp}(t)$ and $C''_{calc}(t)$ is made by the

Table 1. Geometric characteristics of the particles and the fixed beds

Type	*Material*	ϱ (*kg m*$^{-3}$)	*Thickness* e (*mm*)	*Side* a (*mm*)	e/a	a_{vs} (*m*$^{-1}$)	ε
Flat plates	Polystyrene	1050	0.517	5.050	0.102	4659	0.46
	PVC	1467	1.045	5.00	0.209	2713	0.35
	PVC	1485	2.18	4.96	0.440	1724	0.31
Glass beads	d_p = 4.99 × 10^{-3} m						
	a_{vs} = 1203 m^{-1}						
	ε = 0.40						

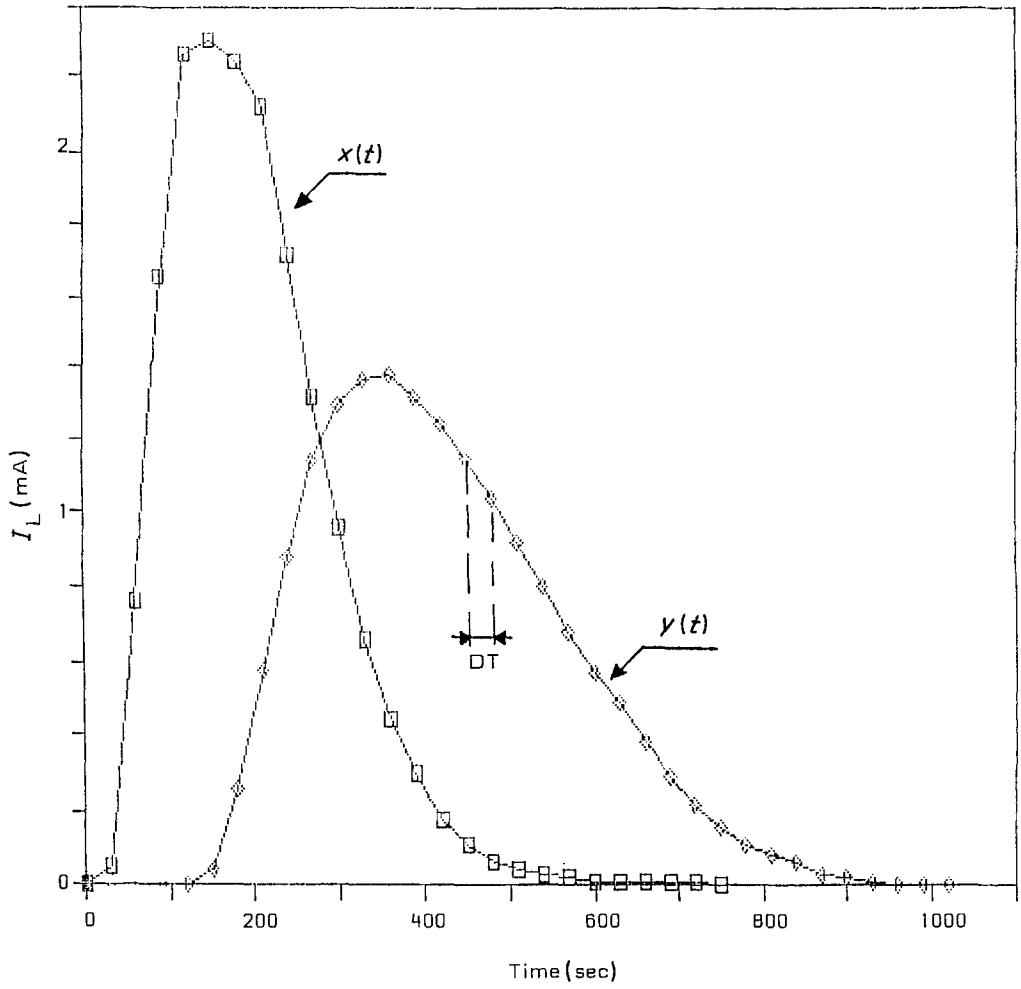

Fig. 3. Experimental curves obtained with a fixed bed of flat plates with $e/a = 0.102$ and for mass flow rate equal to $9.75 \times 10^{-4}\,\mathrm{kg\,s^{-1}}$.

evaluation [4] of the root mean square error ER:

$$\mathrm{ER} = \left[\frac{\int_0^{2T} [C''_{\mathrm{exp}}(t) - C''_{\mathrm{calc}}(t)]^2 \, \mathrm{d}t}{\int_0^{2T} [C''_{\mathrm{exp}}(t)]^2 \, \mathrm{d}t} \right]^{1/2} \quad (8)$$

ER is a function of Pe and $\bar{t}_s$. The minimum of the function ER is sought by the optimization method of Hooke and Jeeves [7]. The desired parameters $\bar{t}_s$ and Pe, and then the axial dispersion coefficient D_{ax}, satisfy the relation ER < 0.05 to have a good fitting [4].

4. Experimental results

4.1. *Fixed bed of spherical particles*

There are numerous studies of axial dispersion in fixed beds of spherical particles [8]. We have chosen this type of packed bed in order to test the electrochemical method for the determination of the RTD. The studied fixed bed is composed of glass beads 4.99 mm in diameter and the porosity of the bed is 0.40.

In Fig. 4 we have shown our experimental results in the diagram established by Chen and Wen [8] from 13 different papers dealing with liquid phase dispersion in fixed beds. Figure 4 gives the variation of εPe_i vs Reynolds number Re, based on the superficial velocity u_0. Our data are in accordance with those of the literature. We can conclude that the electrochemical method can be performed with good accuracy for the determination of axial dispersion in fixed beds.

Our experimental data can be correlated by the following equation:

$$Pe_i = 0.74 Re_i^{0.03} \quad (9)$$

with a relative mean square error

$$\mathrm{RMSE} = \left[\frac{1}{n} \sum_1^n \left(\frac{Pe_i(\mathrm{meas}) - Pe_i(\mathrm{calc})}{Pe_i(\mathrm{meas})} \right)^2 \right]^{1/2}$$

equal to 0.14. The Peclet and Reynolds numbers are based on the interstitial velocity u. The Reynolds number, Re_i, varies between 2.6 and 75.3.

Equation 9, obtained with an isotropic fixed bed, will be used to make a comparison with the anisotropic fixed beds composed of flat plates.

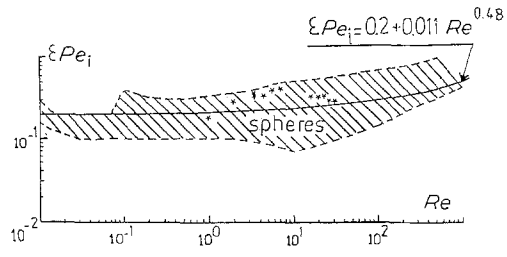

Fig. 4. Comparison of the results obtained with the fixed bed of glass beads with the literature data (after [8]).

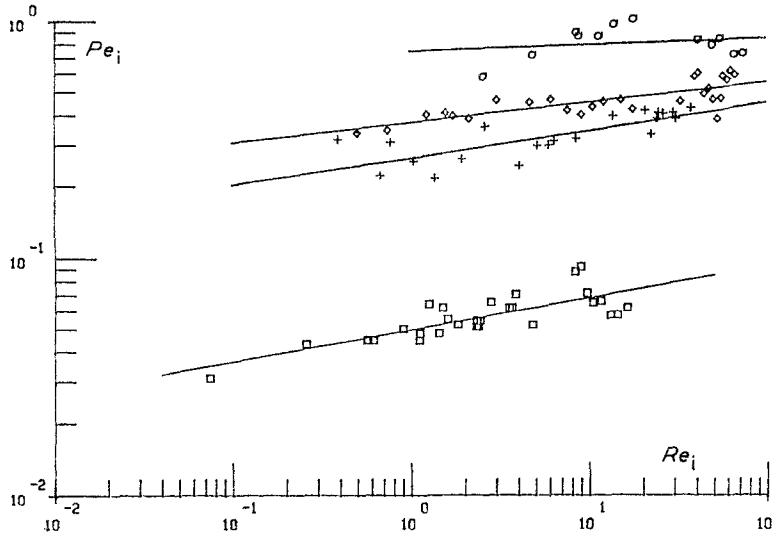

Fig. 5. Pe_i vs Re_i for flat plates and spheres: □ $e/a = 0.102$, $Pe_i = 0.049Re_i^{0.14}$; + $e/a = 0.209$, $Pe_i = 0.26Re_i^{0.12}$; ◇ $e/a = 0.440$, $Pe_i = 0.35Re_i^{0.08}$; ○ spheres, $Pe_i = 0.74Re_i^{0.03}$.

4.2. *Fixed beds of flat plates*

The experimental data are expressed in terms of Peclet numbers, Pe_i, as a function of Reynolds number, Re_i, (Figure 5). The two adimensional numbers are based on the equivalent diameter defined by $d_p = 6/a_{vs}$.

The results are correlated by different expressions according to the geometrical characteristics of flat plates:

with $0.07 < Re_i < 16.2$

$$e/a = 0.102,\ Pe_i = 0.049Re_i^{0.14}\ (\text{RSME} = 0.14) \tag{10}$$

with $0.39 < Re_i < 38.1$

$$e/a = 0.209,\ Pe_i = 0.26Re_i^{0.12}\ (\text{RSME} = 0.14) \tag{11}$$

with $0.50 < Re_i < 66.3$

$$e/a = 0.440,\ Pe_i = 0.35Re_i^{0.08}\ (\text{RSME} = 0.10) \tag{12}$$

In Fig. 5 we can see that the Peclet number is greater, and consequently the axial dispersion coefficient lower, in fixed beds of spheres than in those of flat plates. For flat plates, the Peclet number decreases with the geometric ratio e/a (Fig. 5). We also note the particular behaviour of the thinnest flat plates ($e/a = 0.102$); indeed, for these particles the axial dispersion coefficients are very significant, about 10 times greater than those obtained with the spherical particles (Fig. 5). This difference can be explained by the flow pattern around the particles inside the fixed beds. For the beds of spherical particles, the fluid divides and flows around the spheres (Fig. 6) with slip at the surface. For tightly packed beds of flat plates, the mean orientation of the parallelipipedic particles is nearly perpendicular to the flow direction [3]. So, we can assume that jet-type flow occurs (Fig. 6) when the fluid elements meet the main face of the plates. Consequently, backmixing is promoted and thus the axial dispersion is enhanced. The thinner the flat plates, the greater the mixing due to more frequent direction shifts and the larger number of flat plate layers. The axial dispersion coefficient characterizes the degree of backmixing superimposed on plug flow. Increase of the axial dispersion is due to the increase of the flow velocity fluctuations inside the porous medium [9, 10].

5. Discussion

The behaviour of the packed beds of flat plates may be assessed by using the equation obtained by Gunn [11, 12] from the description of axial mixing by stochastic processes and probability theory. Gunn has represented the convective motion by the probability of a tracer particle either remaining at rest or travelling a distance downstream. The probability of the tracer particle covering this distance downstream is constant and equal to p: the probability of the tracer particle remaining at rest is $1 - p$. The total displacement of the tracer particle with time is due to both convective and diffusion motions. The analysis of the tracer particle motion leads to the following expression [11, 12]:

$$\frac{1}{Pe_i} = \frac{\varepsilon Re_i Sc}{4\alpha_1^2(1-\varepsilon)}(1-p)^2 + \frac{Re_i^2 Sc^2 \varepsilon^2}{16\alpha_1^4(1-\varepsilon)^2}p(1-p)^3 \times \exp\left(\frac{-4(1-\varepsilon)\alpha_1^2}{p(1-p)\varepsilon Re_i Sc} - 1\right) + \frac{1}{\tau Re_i Sc} \tag{13}$$

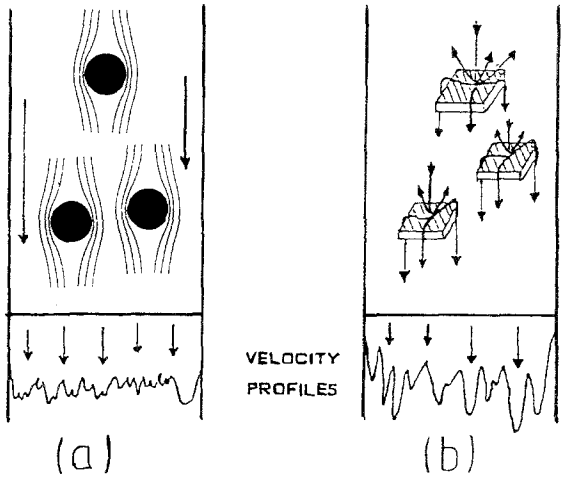

Fig. 6. Schematic flow pattern for flows through: (a) fixed beds of spheres; (b) fixed beds of flat plates.

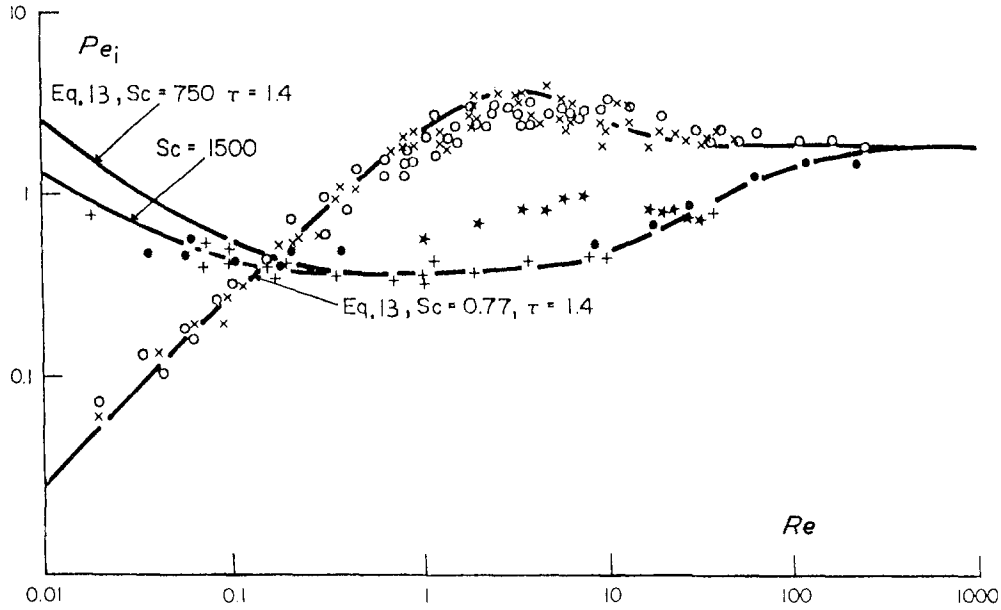

Fig. 7. Comparison (after Gunn [12]) of experimental measurements for axial dispersion in beds of spheres with $p = 0.17 + 0.33 \exp(-24/Re_i)$: gas phase: o, Gunn and Pryce [13]; ×, Edwards and Richardson [2]; liquid phase: ●, Jacques and Vermeulen (cited by Gunn [12]); +, Miller and King [14]; ★, our data for spheres of 0.5 cm diameter.

where $\alpha_1 = 2.40483$ is the first root of first order Bessel function and τ the tortuosity factor. The interest of Equation 13 is that it correctly describes the gas phase and liquid phase mixing data (Fig. 7). In particular, for the liquid phase and for Reynolds numbers Re_i less than 0.5, Equation 13 gives a decrease in Peclet number with an increase in Reynolds number. This behaviour is the same as that obtained in a tube for the laminar flow regime [1]. This result confirms the prediction of Edwards and Richardson [2] who have noted that the difference between the axial dispersion in the gas phase and the liquid phase is due to the presence of a laminar flow regime in the liquid phase, which is absent in the gas phase where the diffusion process dominates up to moderate values of Reynolds number. For a large domain of Reynolds number, Gunn [12] has obtained a variation of the probability p between 0.17 and 0.50 for beds of spheres, between 0.17 and 0.46 for beds of solid cylinders and between 0.17 and 0.37 for beds of hollow cylinders: the probability, p, decreases with the anisotropy of the particles. The results obtained with beds of spheres of 5 mm diameter are reported in Fig. 7. The data are rather different from those predicted by Equation 13, but this can be explained by the fact that the experimental points for the liquid phase dispersion are more scattered (see Fig. 4) than indicated by Gunn [12]. For the beds of flat plates we have obtained a variation of the probability p between 0.012 and 0.044 for $e/a = 0.102$, between 0.087 and 0.17 for $e/a = 0.209$ and between 0.12 and 0.23 for $e/a = 0.44$. The values of p obtained for flat plates are lower than those for spheres and cylinders. The weakness of the probability p is associated with important variations of the velocity within a cross section. The results confirm the fact that the flow is more perturbed in flat plate beds than in more isotropic particle beds, and the flow is the more perturbed as the flat plates are thinner.

This result may also be interpreted by modelling fixed beds as an array of parallel cylindrical pores of different diameters [15]. Carbonell [15] has characterized the dispersion in porous media with a simple model taking into account the pore size distribution and the flow regime. He has considered an array of N straight parallel pores; each pore has a radius r and an area-averaged fluid velocity u. This model is expressed as:

$$D_{ax} = \sum_{i=1}^{N} D_{ax_i}\omega_i + \bar{r}\sum_{i=1}^{N} \bar{u}_{ti}\omega_i\left(\frac{\bar{u}_{ti}}{\bar{u}_t} - 1\right) \quad (14)$$

where D_{ax} is the mean dispersion coefficient in the porous media, D_{ax_i} the dispersion coefficient in the pore i. Assuming cylindrical pores, the mean radius pore $\bar{r}$ is defined by:

$$\bar{r} = \frac{2\varepsilon}{a_{vs}(1-\varepsilon)} \quad (15)$$

and the fraction ω_i of the total solute present in the pore i by:

$$\omega_i = \frac{\bar{u}_{ti} r_i^2}{\bar{u}_t \sum_{i=1}^{N} r_i^2} \quad (16)$$

where $\bar{u}_t = u_0\tau/\varepsilon$ is the area-averaged fluid velocity in the porous medium. For the laminar flow regime, the dispersion coefficient in a tube is given by Aris [16] as

$$D_{ax_i} = D + \frac{\bar{u}_{ti}^2 r_i^2}{48D} \quad (17)$$

The mean fluid velocity, $\bar{u}_{ti}$, in the pore i is given by the

Hagen–Poiseuille equation:

$$\bar{u}_{ti} = \frac{r_i^2}{8\mu}\frac{\Delta P}{L} \tag{18}$$

The velocity $\bar{u}_t$ is defined by:

$$\bar{u}_t = \frac{\sum_{i=1}^{N} \bar{u}_{ti} r_i^2}{\sum_{i=1}^{N} r_i^2} \tag{19}$$

From Equations 14, 16 and 19, Carbonell [15] has obtained the following equation for the mean dispersion coefficient in the laminar regime:

$$D_{ax} = D + \frac{\bar{u}_t^2}{48D}\frac{\overline{r^{10}}\,(\overline{r^2})^2}{(\overline{r^4})^3} + \bar{u}_t\bar{r}\frac{\overline{r^2}}{(\overline{r^4})^2}\left(\frac{\overline{r^2}\,\overline{r^8}}{\overline{r^4}} - \overline{r^6}\right) \tag{20}$$

where

$$\overline{r^n} = \frac{1}{N}\sum_{i=1} r_i^n$$

is the nth moment of the pore size distribution. Carbonell has assumed that the pore size distribution may be described by a Gaussian distribution with standard deviation σ; Equation 20 becomes:

$$\frac{1}{Pe_t} = \frac{1}{Re_t Sc} + \frac{Re_t Sc}{96} f_1(\gamma) + \frac{f_2(\gamma)}{2} \tag{21}$$

where $\gamma = \sigma/\bar{r}$ is the variation coefficient, and the functions f_1 and f_2 are given by Carbonell [15]. As $\gamma \to 0$, all the pores have the same radius $\bar{r}$.

For the turbulent flow regime, the dispersion coefficient in a tube has been determined by Taylor [17]:

$$D_{ax_i} = 10.1 r_i \bar{u}_{ti}\sqrt{f/2} \tag{22}$$

where f is the friction factor represented by the Blasius formula:

$$f = 0.316 Re_t^{-1/4} \tag{23}$$

From Equations 14, 22 and 23, Carbonell has obtained, for the mean dispersion coefficient in turbulent regime, the following expression:

$$D_{ax} = 1.8407 \nu^{1/8}\bar{u}_t^{7/8}\frac{\overline{r^{59/14}}\,(\overline{r^2})^{7/8}}{(\overline{r^{19/7}})^{15/8}} + \bar{u}_t\bar{r}\frac{\overline{r^2}}{(\overline{r^{19/7}})^2}\left(\frac{\overline{r^2}\,\overline{r^{29/7}}}{\overline{r^{19/7}}} - \overline{r^{24/7}}\right) \tag{24}$$

As for the laminar flow regime, we can express the axial dispersion in terms of Peclet number Pe_t:

$$\frac{1}{Pe_t} = 1.0036 Re_t^{1/8} g_1(\gamma) + \frac{g_2(\gamma)}{2} \tag{25}$$

Figure 8 shows Pe_t vs Re_t for the present experimental results. The axial dispersion data are well represented by Equation 25 with $\gamma = 1.0$ for the spheres, $\gamma = 1.7$ for the flat plates with $e/a = 0.209$ and 0.440 and $\gamma = 3.0$ for the flat plates with $e/a = 0.109$. The increase of the axial dispersion is expressed by the increase of γ. Consequently, the pore size distribution is greater when the anisotropy of the porous medium increases. In Fig. 8 it can be noted that the laminar regime is obtained for very low Reynolds number, Re_t. From a dispersion point of view, the flow through fixed beds is similar to turbulent flow, and the promotion of the turbulence is greater with more anisotropic particles.

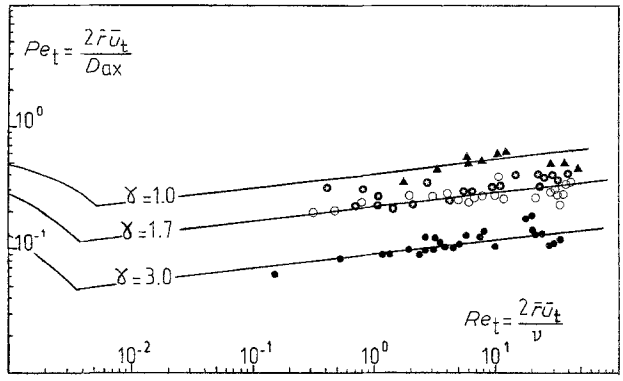

Fig. 8. Comparison of the experimental data with the pore size distribution model: ▲, spheres with $d_p = 0.5$ cm; ○, flat plates with $e/a = 0.440$; ●, flat plates with $e/a = 0.209$; ●, flat plates with $e/a = 0.102$.

6. Conclusion

Axial dispersion measurements were performed using an electrochemical method in fixed beds of flat plates which constitute anisotropic porous media. The experimental results have shown that axial dispersion coefficients are greater with fixed beds of flat plates than with fixed beds of spheres. Experimental correlations giving Peclet number as a function of Reynolds number for fixed beds of different thickness-to-side ratio are proposed, and it is noticed that axial mixing clearly increases when this ratio decreases. From the axial dispersion point of view, the particular behaviour of the fixed beds of flat plates, by comparison with beds of spheres, is explained by more significant velocity fluctuations within a cross section. This result has been quantified using the stochastic model of Gunn and with the pore size distribution model of Carbonell.

References

[1] C. Y. Wen and L. T. Fan, 'Models for Flow Systems and Chemical Reactors', Dekker, New York (1975).
[2] M. F. Edwards and J. F. Richardson, *Chem. Eng. Sci.* **23** (1968) 109.
[3] J. Comiti, Thesis, Grenoble (1987).
[4] N. Wakao and S. Kaguei, 'Heat and Mass Transfer in Packed Beds', Gordon and Breach, London (1982).
[5] W. C. Clements, *Chem. Eng. Sci.* **25** (1969) 957.
[6] M. A. Fahim and N. Wakao, *Chem. Eng. J.* **25** (1982) 1.
[7] G. S. G. Beveridge and R. S. Schechter, 'Optimization: Theory and Practice', MacGraw Hill, New York (1970).
[8] S. F. Chen and C. Y. Wen, *A.I.Ch.E. J.* **14** (1968) 857.
[9] J. L. Stephenson and W. E. Steward, *Chem. Eng. Sci.* **41** (1986) 2161.
[10] S. A. Volkow, V. I. Reznikow, K. F. Khalilov, V. Yu. Zel'Vensky and K. I. Sakodynsky, *Chem. Eng. Sci.* **41** (1986) 389.

[11] D. J. Gunn, *Trans. Inst. Chem. Engrs* **47** (1969) T351.
[12] D. J. Gunn, *Chem. Eng. Sci.* **42** (1987) 363.
[13] D. J. Gunn and C. Pryce, *Trans. Inst. Chem. Engrs* **47** (1969) T 341.
[14] S. F. Miller and C. J. King, *A.I.Ch.E. J.* **12** (1966) 767.
[15] R. G. Carbonell, *Chem. Eng. Sci.* **34** (1979) 1031.
[16] R. Aris, *Proc. R. Soc. London* **A235** (1956) 67.
[17] G. I. Taylor, *Proc. R. Soc. London* **A223** (1954) 446.